

Numerical approach of the steel-concrete bond behavior using pull-out models

Fernando Menezes de Almeida Filho¹, Silvana De Nardin¹,
Ana Lúcia Homce de Cresce El Debs²

¹ Professor, Programa de Pós-graduação em Estruturas e Construção Civil – PPGE Civ, DECiv/UFSCar, Rod. Washington Luis, km 235, São Carlos, São Paulo, Brasil.

² EESC/USP - Departamento de Engenharia de Estruturas - Av. Trabalhador São-carlense, 400, São Carlos, São Paulo, Brasil.

e-mail: almeidafilho@ufscar.br, snardin@ufscar.br, analucia@sc.usp.br

ABSTRACT

This paper deals with the analysis of monotonic loading behavior in pull-out tests. The main objective is to obtain a reliable numerical model to represent the steel-concrete bond behavior using previously obtained experimental results. The tests were performed in RILEM pull-out specimen using 10 mm steel bar and concrete with compressive strength of 30 MPa. The numerical study used Ansys® software, based on FEM (Finite Elements Method). The numerical simulation adopted non-linear constitutive relationships to represent the behavior of both concrete and steel. A contact surface composed of special finite elements modeled the interface between the concrete and the steel bar, allowing a steel-concrete slip. The numerical analysis performed with variation of the main parameters of the software permitted determining the best ones, and choosing them to obtain a good representation of the bond phenomena. The numerical results had a good agreement with the experimental results. Both linear and non-linear approaches represented the pre-peak behavior, however only the non-linear model gave the best approach for the pull-out force. In addition, the numerical results had shown the simplified model can be used to represent the steel-concrete bond behavior reducing the processing time for current structures analysis.

Keywords: bond strength, pull-out tests, numerical approach, contact surface, finite element method.

1. INTRODUCTION

Reinforced concrete is a composite structure made by two different materials with its characteristics, specifically, concrete and steel. The application of the loads on a structure, rarely, is directly applied on the reinforcement and, the surrounding concrete makes the transition of the actions applied. The bond stress is the phenomena responsible by the load transfer from the concrete to the steel. The bond, when efficiently developed, enables these two materials to form a composite structure.

The pull-out of a steel bar from a concrete prism involves the rupture of the concrete adjacent to the steel bar and, according to NIELSEN [1], a mechanism with pure slip would not be possible. It occurs in function of the concrete expansion resulting from the radial deformation that appears in the transfer of efforts responsible for the sliding of the bar. The tension in the steel bar provokes the increase of stress in concrete struts, producing circumferential tension stresses. Therefore, if a steel bar is located close to the concrete prism surface, the splitting of concrete will occur. Likewise, if there is no reinforcement in the concrete prism, the bond resistance will depend almost totally on the concrete strength.

According to BANGASH [2], the bond stress varies in function of three portions. The first one is the adhesion, which consists of the resistance against shear between concrete and steel; the second is the frictional coefficient, which is a decisive factor for the bond resistance in elements at the ultimate limit state; the last portion is the interaction between the materials (bearing action), which is caused by the deformation of the bars in contact with the concrete.

The bond mechanism involves four components (LUNDGREN *et al.* [3]): friction, normal stress on slip, adhesion and failure of the concrete between the steel bar ribs. There are several types of failure associated to the loss of bond between the concrete and the steel bar, and the main ones are pull-out failure

and splitting failure. These failures are strongly influenced by several factors, such as type of reinforcement (bar, tendons and strings), superficial characteristics (flat or rough), diameter of the bar, presence of confinement reinforcement, distance among the bars, cover, steel bar stress, concrete quality and others.

According to FERGUSON [4], when the slip of the steel bar reaches the whole extension of the embedment length in pullout tests, three failure types may occur: longitudinal splitting of the concrete, pull-out of the steel bar (in the case of shorter diameters or using low strength concrete), and slip of the steel bar when the embedment length is enough. There are four types of different mechanisms in the bond phenomenon: elastic deformation, secondary cracks, cracks caused by the longitudinal splitting, and concrete crush at the ribs of the steel bar (ROTS [5]). Fig. 1 shows these mechanisms.

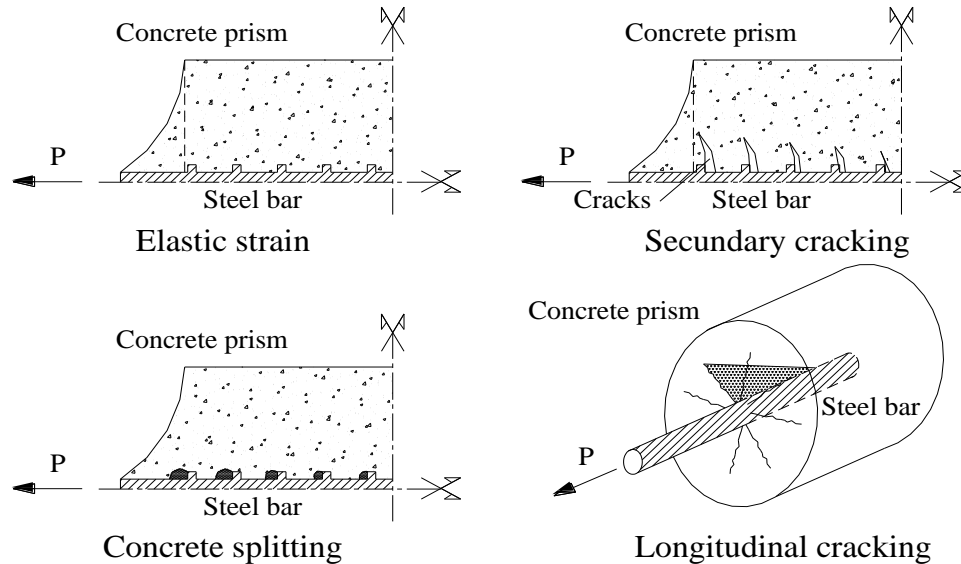


Figure 1: Bond mechanism failures (adapted from Rots [5]).

According to the referred author, the portion regarding the steel bar behavior discussed by AL-JAHDALI *et al.* [6] is missing. Likewise, in a simple pull-out test without adding confinement reinforcement or steel fibers, four modes of failure may occur:

- Pull-out: consists in the slipping of the steel bar from the concrete prism, as the concrete cover adjacent to the steel bar promotes an appropriate confinement preventing the splitting of the model, characterizing a ductile failure.
- Splitting: consists in the failure of the concrete adjacent to the steel bar. It occurs because of the increase in the stress that overcomes the capacity of the element, originating an intense cracking in the transverse and longitudinal directions. This mode of failure is characterized as fragile.
- Tension: consists in the formation of cracks perpendicular to the load direction, at the embedded extremity of the steel bar.
- Steel failure: consists in the steel bar yielding before the connection capacity between steel and concrete has been reached; in other words, the bond stress among the two materials exceeds the yield limit of the steel bar.

The bond resistance results from a shear stress that acts parallel to the steel bar, in the contact zone between the bar and the adjacent concrete. The stress varies along the steel bar due to the transfer of efforts between the steel bar and the adjacent concrete. The load applied to the bar goes to the concrete through radial forces that appear along the bar, and the bond stresses will vary according to the amount of load per area transmitted from the steel bar to the involving concrete. Therefore, the bond stress appears only if there is a

force variation along the steel bar (KWAK and KIM [7]). The bond stress vs. slip behavior in a pull-out test and the bond stress in the steel bar are shown in Fig. 2.

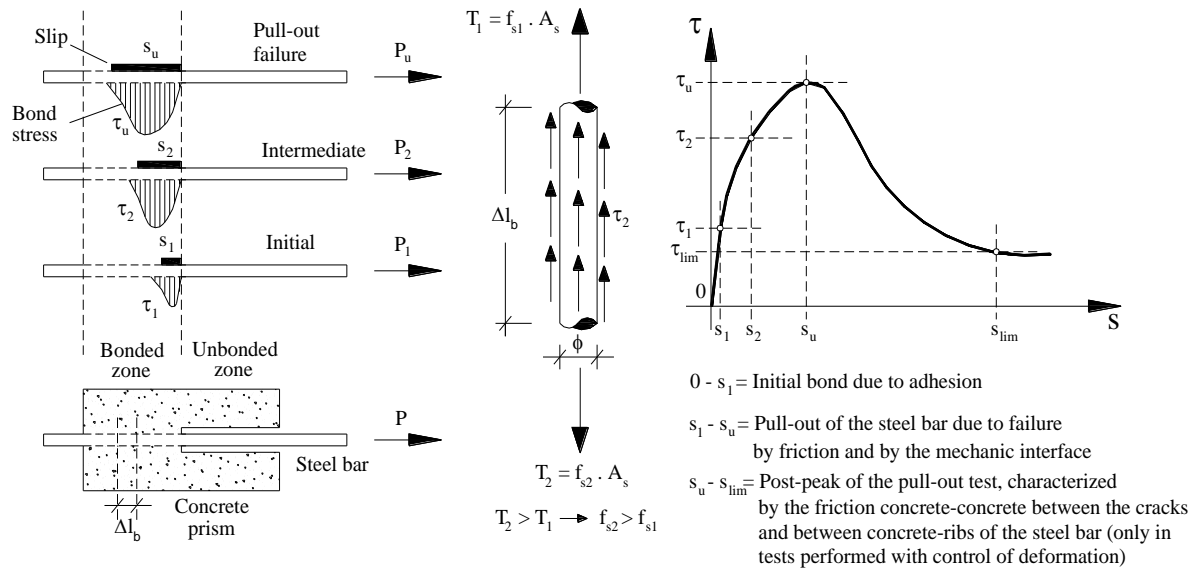


Figure 2: Bond stress and slip behavior in a pull-out test.

The failure in the steel-concrete interface could be attained by combining Coulomb’s frictional hypothesis with a bound for the maximum tensile stress (Fig. 3), resulting in two different failure modes that could be called sliding failure and separation failure (NIELSEN [1]). The sliding failure is assumed to occur in a section when the shear stress exceeds the sliding resistance and should be determined by two parameters: cohesion © and friction coefficient (μ).

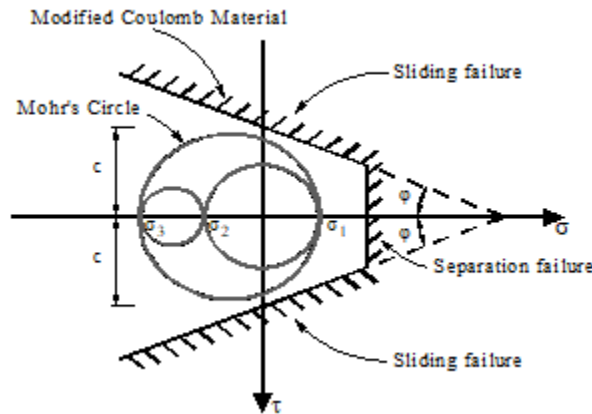


Figure 3: Modified Mohr-Coulomb material behavior (adapted from NIELSEN [1]).

Eq. 1 obtains the cohesion (c) and the friction coefficient (μ).

$$f_c = 2 \cdot c \cdot \sqrt{k} \text{ and } k = \left(\mu + \sqrt{1 + \mu^2} \right)^2 \quad (01)$$

In agreement with the literature (NIELSEN [1]), for low strength concrete and if concrete is identified

as a modified Mohr-Coulomb material, parameter “ k ” has a value around 4. Therefore, the value of μ will be 0.75, which corresponds to a friction angle of 37° and leads to cohesion of 0.75 kN/cm^2 .

The determination of the bond strength is made, usually, by pull-out tests. The theoretical behavior is shown in Figure 4.

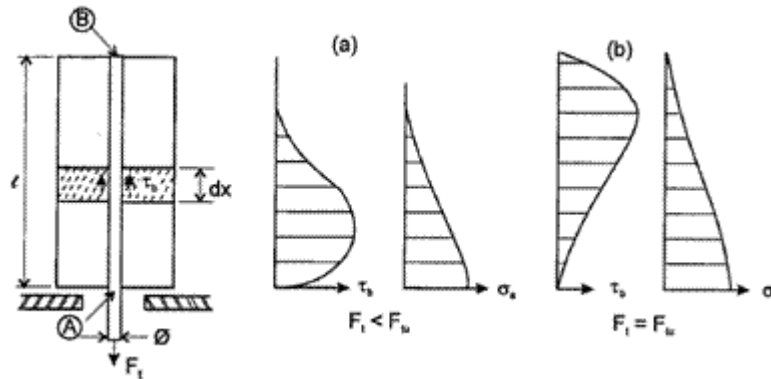


Figure 4: Bond stress distribution in a pull-out test (FUSCO [8]).

In Figure 4a, the bond stress distribution is shown for a force applied (F_t) lower than the rupture force, showing the bond strength at the concrete interface and the steel interface. The same is shown in Figure 4b when the force applied (F_t) reaches the rupture force (F_u). In both cases, the bond stress varies showing the concrete contact strength distribution.

For the numerical simulation of the steel-concrete interface, several studies were developed, where could be emphasized the constitutive law of the two materials. According to the literature, several finite elements present a better evaluation of the bond behavior, but there is still the absence of an adequate constitutive law that may represent the bond phenomena. The steel-concrete interface consists of a discontinuous surface, made by a contact surface of two materials and that behavior depends on the used materials (DÉSIR *et al.* [9]; KWAK and KIM [7]; SALARI and SPACONE [10]; KWAK and FILIPPOU [11]; YANKELEVSKY [12]; GIRARD and BASTIEN [13]; KOTSOVOS and PAVLOVIC [14]; DEHESTANI and MOUSAVI [15], HASKETT *et al.* [16], BRISOTTO *et al.* [17]).

1.1 Objectives and research significance

The main objective here is to evaluate the bond-slip behavior and the bond stress on the steel bar, analyzing the influence of the parameters considered by FEM software, in this case, ANSYS [18]. The results provided by the numerical analysis were compared to the experimental one given by FERNANDES [19]. Also, the present paper aims to contribute to the better understanding of the bond stress behavior and furnish numerical data for future researchers.

The steel-concrete bond is one of the most difficult problems to face in the study of reinforced concrete and researchers still does not completely understand its behavior. It occurs due to the great number of parameters needed to represent the bond phenomena, making the study of bond behavior very important. Besides, the numerical modeling of bond, which is a contact problem, is very hard to be performed, as shown by several researchers.

2. MATERIALS AND EXPERIMENTAL PROGRAM

The tests were performed by FERNANDES [19]. The tested specimens had steel bars with 10 mm or 20 mm diameter, and a concrete compressive strength of 30 MPa, at 28 days. Fig. 5a shows the geometry of the pull-out specimens after failure. As expected, the rupture mode was the pull-out of the steel bar, due to the concrete presented low compressive strength and the development length of the RILEM model. After the performed test, the concrete cylinder was cut in a half for the evaluation of the concrete internal cracks on its longitudinal section (Fig. 5b).

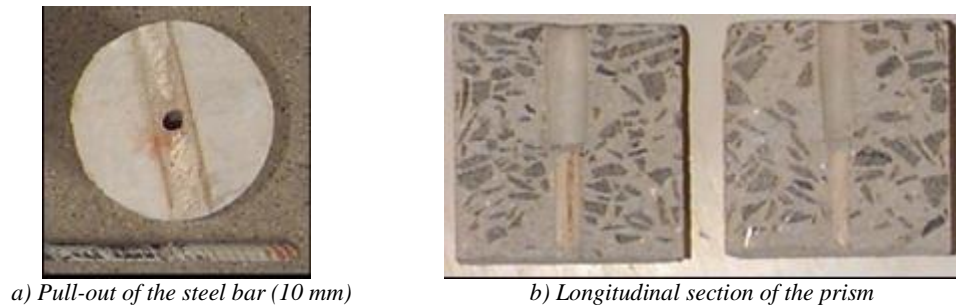


Figure 5: Rupture mode of the pull-out specimen and development length (FERNANDES [19]).

According to the specimen used in this research, the rupture occurred by steel bar slippage. The behavior of the descending branch (post-peak) of the pull-out test curve was soft showing that the steel-concrete interface still influenced the bond behavior (Fig. 6).

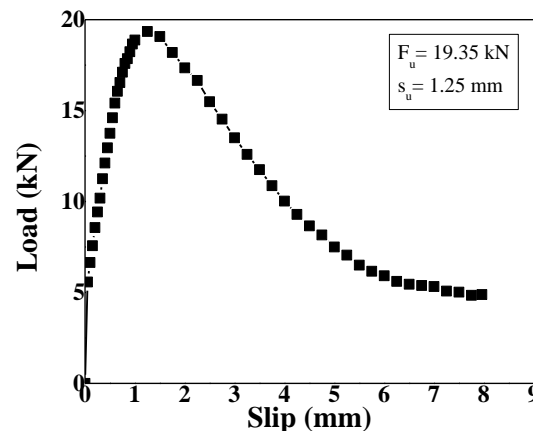


Figure 6: Load vs. slip behavior of the pull-out test (adapted from FERNANDES [19]).

3. NUMERICAL SIMULATION

A numerical model to predict the behavior of the specimens in pull-out tests was developed as part of this study. This model was based on a finite element tool (ANSYS [18]), which admitted non-linear materials behavior (concrete and steel).

3.1 Materials

Compressive strength and modulus of elasticity of the concrete were obtained by tests in cylindrical specimens (10x20cm) and equal to 2,568.0 kN/cm² and the average concrete compressive strength was 2.72 kN/cm². The tension strength of steel bars also was obtained by test results shown in Fig. 6 (assumed in numerical study).

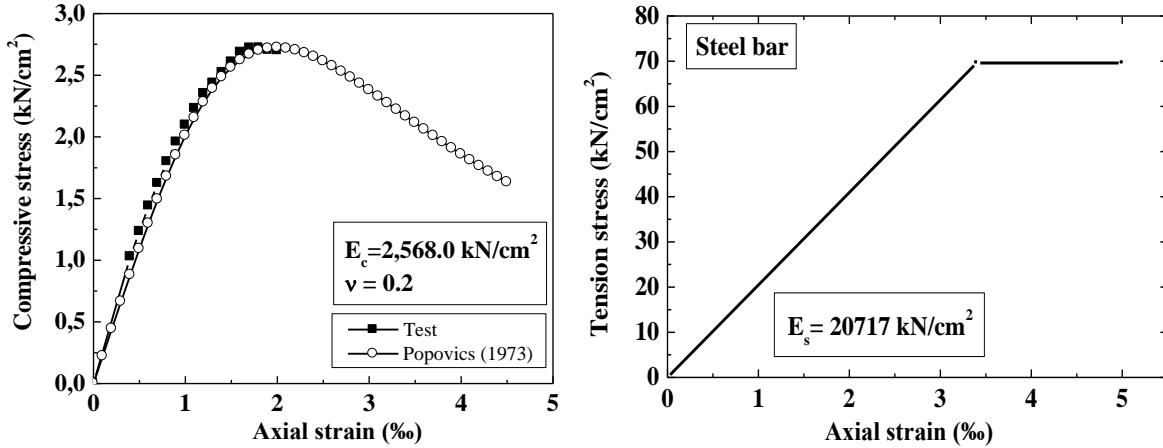


Figure 7: Stress vs. strain behavior of steel and concrete.

There was an absence of the descending branch of the post-peak of its behavior, which could be achieved by using Popovics' formulation (POPOVICS [20]), shown below (Eq. 2).

$$f_c = f_o \cdot \frac{\varepsilon}{\varepsilon_o} \cdot \frac{n}{n - 1 + \left(\frac{\varepsilon}{\varepsilon_o}\right)^n} \quad (02)$$

$$n = 0.4 \cdot 10^{-3} \cdot f_o + 1.0 \text{ and } \varepsilon_o = 2.7 \cdot 10^{-4} \cdot \sqrt[4]{f_o}$$

This formulation takes into account the variation of the concrete compressive strength in the post-peak branch. According to Popovics' theory, the relation between the initial modulus of elasticity (E_c) and the secant modulus of elasticity (E_{cs}) can vary until 4.0 for normal strength concretes and in 1.3 for high strength concretes.

3.2 Geometry, mesh and finite elements

The experimental investigation of the bond stress vs. slip response was realized using the adapted specimen geometry (RILEM-CEB-FIP [21]) shown in Fig. 8a. It consisted of a steel bar with 10 mm of nominal diameter, anchored in 50 mm embedded length in the concrete cylinder (FERNANDES [19]). In Fig. 8c, the failure of the interface between the steel and the concrete surface is made by combining Coulomb's frictional hypothesis with a bound for the maximum tensile stress. This model is named Modified Mohr-Coulomb and is adopted by the ANSYS [18] software.

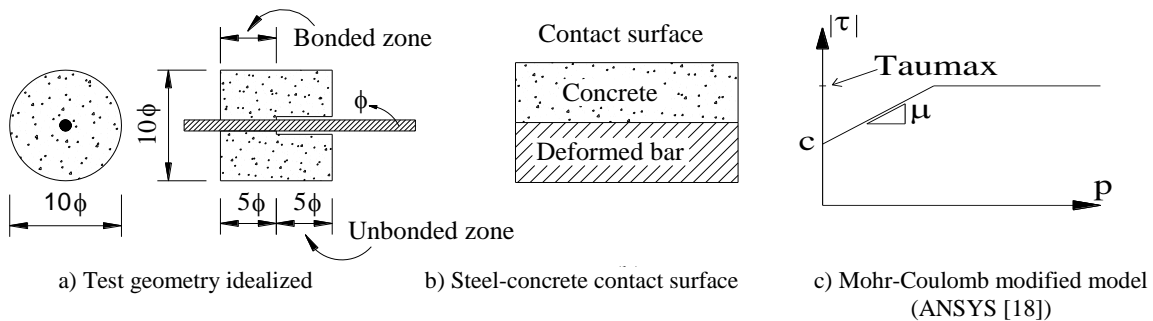


Figure 8: Geometry of the test and contact surface.

The roughness of the steel bars was not considered and a plain contact surface was adopted in the numerical study (Fig. 8b). The finite elements mesh utilized to represent the load vs. slip behavior is shown in Fig 9, and because of the symmetry, a quarter of the pull-out model was studied. The finite element named “Solid65” was used in the numerical analysis to represent the concrete prism and “Solid45” represented the steel bar. In the contact surface a pair of finite elements named “Contal74” and “Targe170” of the Ansys® library was used (ANSYS [18]).

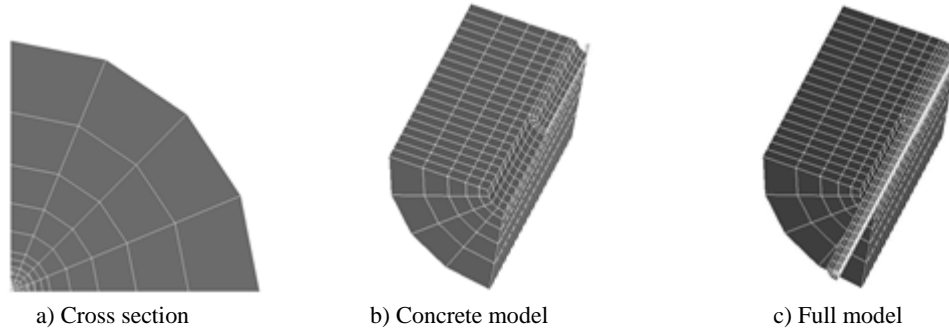


Figure 9: Numerical mesh adopted.

The variables that had more influence on the steel-concrete interface behavior were the chosen for the parametric analysis: normal contact stiffness factor (FKN), tangential contact stiffness factor (FKT), cohesion (c), frictional coefficient (μ) and finite element mesh. Table 1 shows the parameters involved in the linear and non-linear simulations.

Table 1: Numerical parameters

Linear simulation			
<i>Frictional coefficient</i>	<i>Cohesion</i>	<i>Behavior of the contact surface</i>	<i>FKN</i>
0.1	1.357	Standard, Bonded always	0.01; 0.1; 1; 10
0.4	1.015	Bonded, Bonded initial contact	
0.75	0.75	No separation, Rough	
1.0	0.621	No separation always	
Non linear simulation			
<i>Interaction number (IT)</i>	<i>FKN</i>	<i>Behavior of the contact surface</i>	<i>FKT</i>
20, 60, 100, 140	1,3, 5, 7, 10	Bonded, Rough	0.1, 0.3, 0.5, 0.7, 1.0

IT: constant parameters (FKN=10; FKT=0.5) were adopted;

FKN: (FKT=0.5; IT=140);

FKT: (FKN=5; IT=140)

The FKN parameter is defined as the normal contact stiffness factor and the usual factor range is 0.01 to 10 (positive or negative). If the value of FKN is low, the contact surface is more flexible and higher values of FKN correspond to a rigid contact surface. The parameter FKT is defined as the tangent contact stiffness factor and has a default value of 1. The range adopted by the software for this parameter is between 0.1 to 1.

The behavior of the contact surfaces presented in the software and shown in Table 1, is described below.

- *Standard*: represents the unilateral contact, i. e., the normal pressure is equal to zero if the separation happens;
- *Rough*: it models the frictional contact without considering the slip (it adopts $\mu=\infty$);
- *No separation*: the contact surfaces are arrested, but a sliding is possible to occur among the steel and concrete elements, with no separation of the knots;
- *No separation (always)*: there is no separation among contact points that are inside previously to the

penetration area established (pinball region). Also, there is no penetration among the contact elements fixed on the target surface. When there is no penetration, the No separation and No separation always models produce the same results;

- *Bonded*: the contact surface is bonded in all directions;
- *Bonded (always)*: it simulates the separation of the contact points that are initially inside the area of the pre-established penetration (pinball region) or that involve the contact on the target surface along the normal and tangential directions to the contact surface;
- *Bonded (initial contact)*: only the contact elements that are in contact with the target surface at the beginning of the analysis will remain arrested to the objective surface.

3.3 Loading

The geometry and load of the numerical model were similar to the tests (Fig. 9a). The load applied in the test had control of displacement with a rate of 0.005 mm/s. The concrete prism was pushed 8.0 mm from the restricted steel bar (Fig. 9b) in the test. The specimens were subjected to a pull-out displacement of about 1.25 mm, corresponding to the maximum bond stress in the linear model. In the non-linear model 8.0 mm of displacement were applied (maximum displacement of the tests).

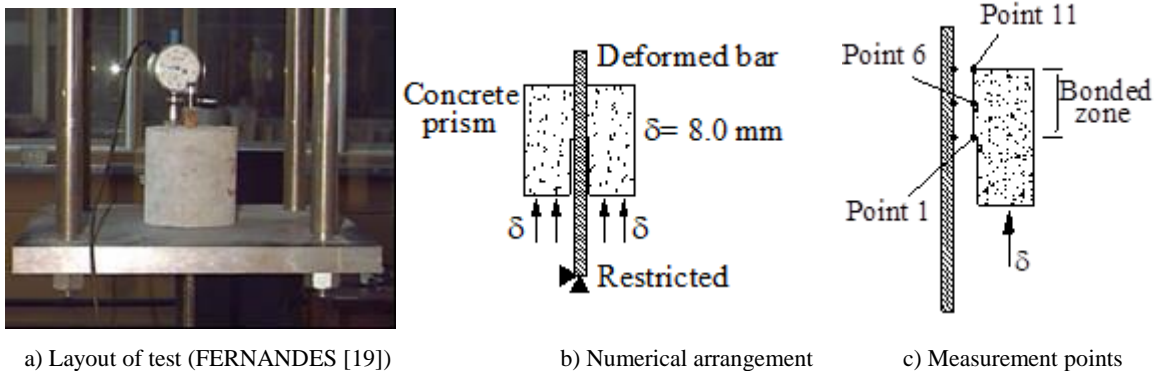


Figure 10: Loading arrangement, numerical arrangement and measurement points.

4. RESULTS AND DISCUSSIONS

This segment presents the analysis between the numerical models and the experimental research made by FERNANDES [19].

4.1 Linear approach

The main idea to develop a linear model was to represent, in a simplified way, the pull-out behavior, using previous test results of pull-out specimens. For the numerical simulation, by varying the FKN value, the same results were found for the contact surface *No separation* and *Standard* (Fig. 10a e Fig. 10b). The models *Bonded (always)*, *Bonded* and *Bonded (initial contact)* produce the same results for the Load vs. Slip behavior, independent of FKN (Fig. 10c). The FKN values between 0.1 and 0.01 probably result in a good approach between numerical and experimental results. For the *Rough* model, the best numerical-experimental approach occurs for FKN=1, whose behavior is similar to the test result (Fig. 10d).

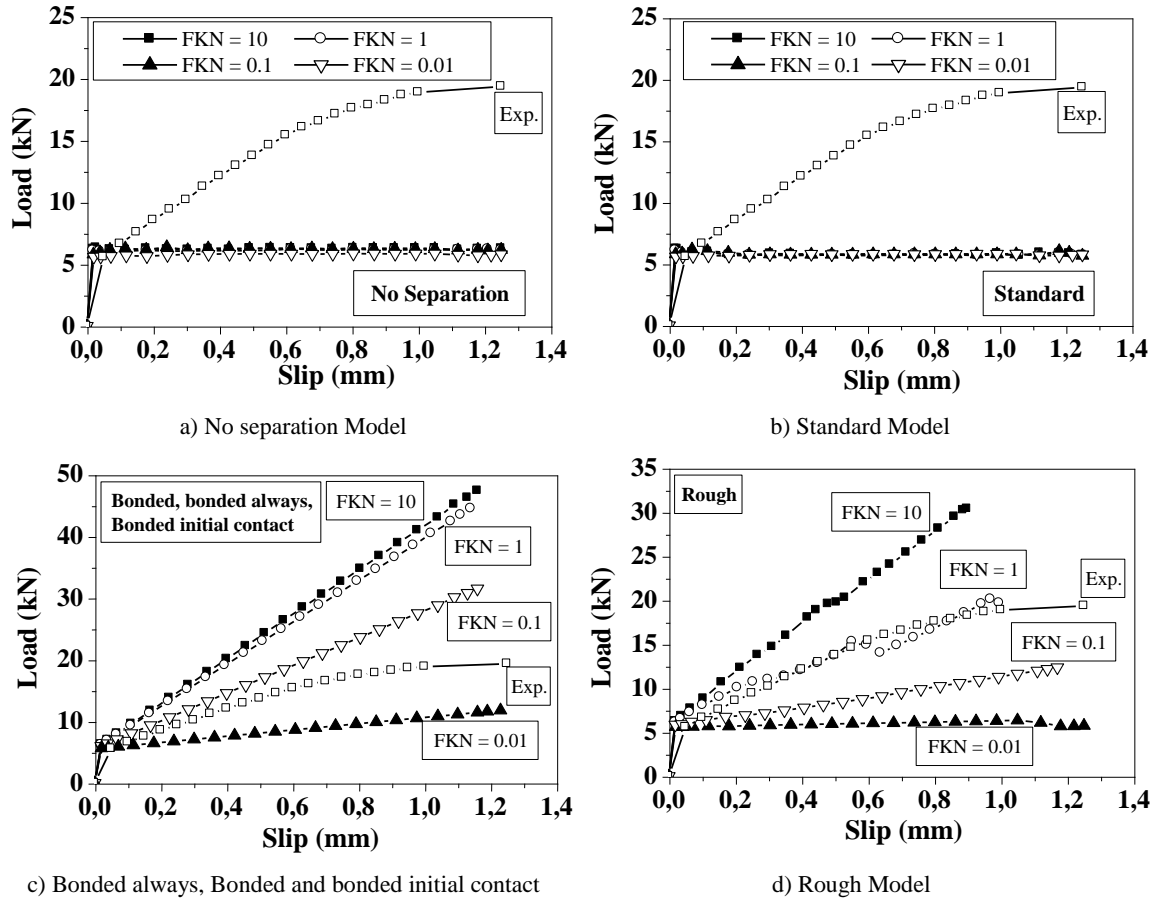


Figure 11: FKN influence on the model of behavior of the contact surface.

There were no changes in the load vs. slip behavior when the frictional coefficient varied (μ) - Fig. 11. The study was realized using *Bonded* and *Rough* models whose results (Fig. 10c and Fig. 10d) show a good agreement with the load vs. slip behavior of the tests.

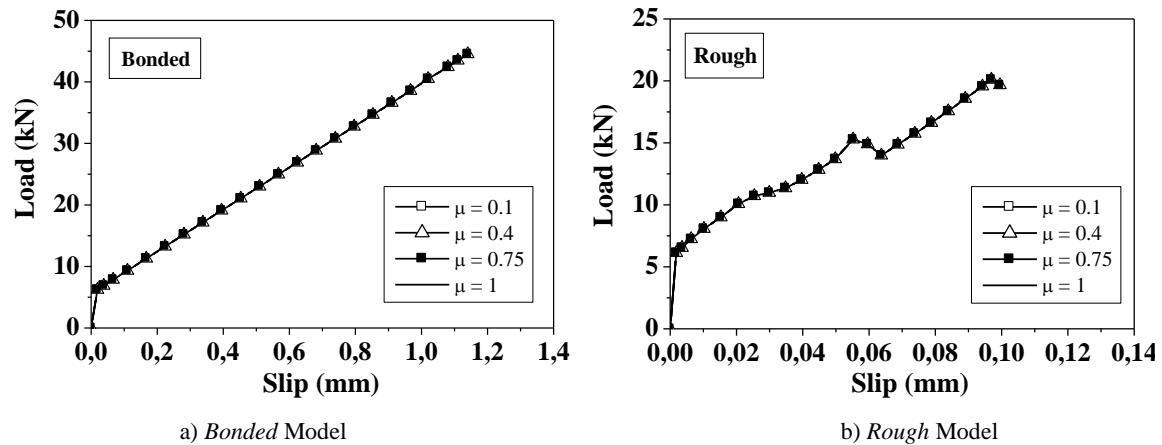


Figure 12: Frictional coefficient and cohesion influence.

There is good agreement of the *Bonded* and *Rough* models to the pre-peak branch of the experimental result (Fig. 11a). According to the formulation of each model of contact behavior, the surface becomes stiffer

than the others, varying the value of FKN.

4.2 Non-linear analysis

The main objective of the non-linear simulation was to represent the pre-peak and post-peak branches of the Load vs. Slip behavior of the pull-out test. In the simulation using ANSYS [18] software, the frictional coefficient was assumed equal to 0.75 and cohesion was 0.75 kN/cm^2 (NIELSEN [1]). The main parameters studied are showed in Table 1 and the bond model adopted was the “bonded contact behavior”. The others models did not show a good result, due to either the large stiffness and/or the large penetration of the contact elements on the contact surface (ALMEIDA FILHO *et al.* [22]; DE NARDIN *et al.* [23]; DE NARDIN *et al.* [24], ALMEIDA FILHO [25]).

According to the parameters shown in Table 1, the number of iterations had an important influence on the response of the numerical model. The short load steps (i.e., large number of iterations) allowed a better approach of the pull-out test behavior only in the pre-peak branch (Fig. 12a). The best result for the load vs. slip behavior was found for 140 iterations. The post-peak branch could not be represented due to the concrete element’s behavior adopted, which do not consider the descending branch on the Stress vs. Strain behavior (Fig. 6) considering Popovic’s theory (POPOVICS [20]). This representation is difficult to make due to several parameters influencing this behavior (ZHOU *et al.* [25]). According to the value of FKN, the pull-out load had a very smooth change, but the value of the slip changed significantly (Fig. 12b). The behavior of the contact surface was very flexible for low values of FKN. The best value for FKN was 5, as it a better agreed with the pull-out test.

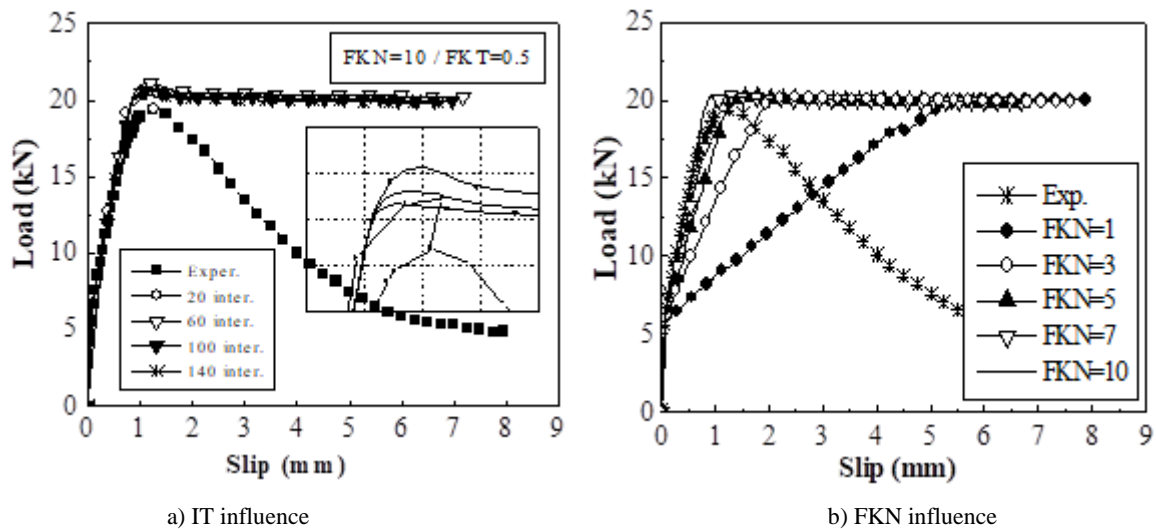


Figure 13: Influence of the number of iterations (IT) and influence of the FKN.

The influence of the FKT is shown in Fig. 13a. The best value obtained for FKN was 5, and was used for the optimization of the FKT parameter, resulting in a better approach with FKT=0.7. Fig. 13b shows the responses of the pull-out load and the bar slip of the test in relation to the numerical results (according to the results of Fig. 13a) confirming the value of FKT adopted (FKT=0.7).

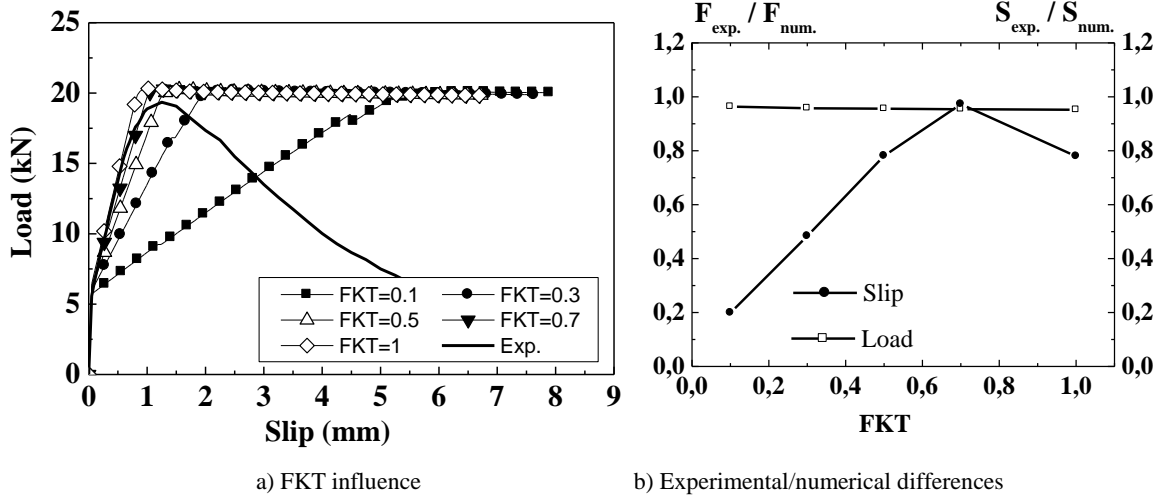


Figure 14: Influence of FKT parameter and differences between test and numerical results.

The variation of the stress on the steel-concrete surface along the slip of the steel bar in the concrete prism is shown in Fig. 14a (for FKN=5 and FKT=0.7). The points of measurement are shown in Fig. 9c. Point 1 had tension stress due to the smaller strength to separation, which can be explained by the shorter concrete length in contact with the steel bar. The other points, especially point 11, show that the concrete was compressed in a crescent way to the end of the embedment length resisting to the steel bar’s slip. Fig. 14b shows the variation of the bond stress at the ultimate load that separates the concrete from the steel bar. The distribution had a good representation of the phenomena, as point 1 had almost zero stress while the maximum stress occurs at point 10, almost at the end of the embedment length. At points 3 and 4, there was a little strength to the slip. The “m” set represents the instant at which the maximum load was reached and, “m-1” and “m+1” represent the instants right before and after of the maximum load, respectively.

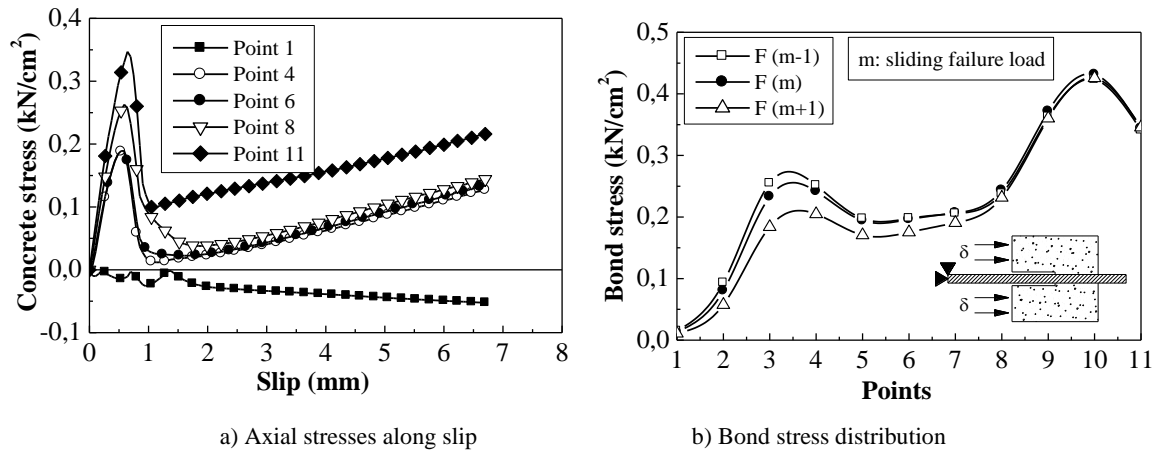


Figure 15: Axial concrete stress and bond stress distribution for the maximum load.

The stress behavior of the adjacent concrete to the steel bar was different for the models studied (Fig. 14b), even when the Load vs. Slip behavior presented a good agreement with the experimental results. The magnitude of the concrete stress for the *Bonded* model was more compatible with the expected response for the test. The value adopted for the *Bonded* model (FKN=0.01) presented the best approach to the expected behavior. Values of FKN in Fig. 12a reach almost 100 MPa for the *Rough* model and almost 12 MPa for the *Bonded* model, and were measured at the end of the embedment length. Although the results of the linear

model had a good agreement to the pre-peak branch, either this model did not represent the post-peak branch due to the linearity of the materials' behavior or the simplified model adopted.

5. CONCLUSIONS

The main objective of this study was to represent the behavior of the steel-concrete interface using the software based on a finite element method. As a simplification, the steel bars did not have any ribs and the behavior of the materials was considered linear and non-linear.

In the linear approach the influence of the contact surface's behavior, the FKN, the frictional coefficient and the cohesion were analyzed. The optimum combination of these parameters was determined, according to the test results. This numerical combination led to good agreement in the pre-peak branch of the load vs. slip test behavior. The main results were:

1. The use of simplified model to represent the behavior of the pull-out test leads to a good Load vs. Slip response to the pre-peak branch;
2. The use of different models of contact behavior present in the software led to different responses, where the best were the *Rough* and *Bonded* models had the best approach;
3. The FKN parameter had a high level of influence on the behavior of the models and each model of contact behavior had an FKN value that led to a better response (Fig. 10);
4. The frictional coefficient and the cohesion were not relevant to the response of the load vs. slip behavior (Fig. 11).

Finally, the values of the numerical parameters depend on the required results. For example, to represent the load vs. slip behavior, it is necessary to use $FKN=0.05$ (*Bonded* model - Fig. 12a) and to represent the value of the concrete stress, it is necessary to use $FKN=0.01$ (Fig. 12b). Therefore, to represent the load vs. slip behavior, both models (*Rough* and *Bonded*) showed good agreement with the experimental results, but to represent the concrete stress the *Bonded* model showed a better behavior using a different value of FKN.

For the non-linear approach, according to the results obtained from the linear approach, it was analyzed the influence of the IT (iteration number), FKN and FKT parameters was analyzed and, the optimum combination of these parameters was determined according to the test results.

This numerical combination led to good agreement in the pre-peak branch to the load vs. slip test behavior. However, the post-peak branch was not well represented due to the absence of the ribs either from the steel bar or the finite elements used. The bond stress was well represented on the embedment length, showing a good distribution to the maximum pull-out load, although it did not have any test results to compare.

The main results of the non-linear approach were:

1. The non-linear approach developed only a good correlation with the test results when the *Bonded* model was adopted. For the *Rough* model, once it had a good correlation in the linear approach, it did not have a single result to represent the test, as it showed a high level of stiffness on the steel-concrete interface;
2. The use of simplified model to represent the behavior of the pull-out test led to a good load vs. slip response;
3. The FKN and FKT parameters had a high level of influence on the behavior of the models;
4. The frictional coefficient and the cohesion were not relevant to the response of the load vs. slip behavior.

The linear (L) and non-linear (NL) analyses were in agreement with the pre-peak branch of the load vs. slip behavior (Fig. 15). However, the linear model due to the limitation of the materials' behavior and the simplicity of the model could not represent the post-peak branch. On the other hand, the non-linear model furnished the pull-out force of the steel-bar.

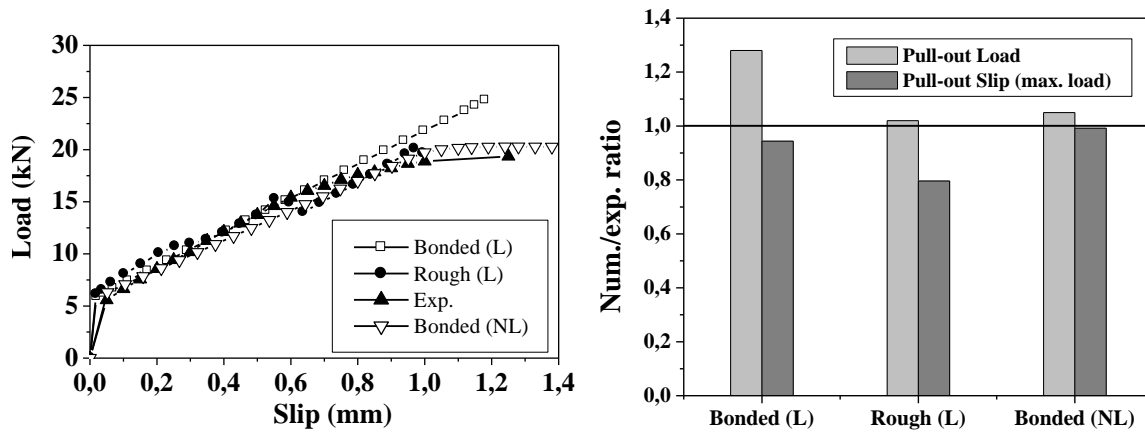


Figure 16: Numerical vs. experimental results.

However, more investigations about the parameters considered in this study and the analysis of other finite elements could be made for a better approach, especially to the post-peak branch in the pull-out test are still necessary, although there were previous studies, it is still a important research that needs attention.

6. ACKNOWLEDGEMENTS

The authors would like to acknowledge FAPESP (Fundação de Amparo à Pesquisa do Estado de São Paulo) and CAPES (Coordenação de Aperfeiçoamento de Pessoal de Nível Superior) for the financial support given to this research.

7. BIBLIOGRAPHY

- [1] NIELSEN, M. P., *Limit analysis and concrete plasticity*, CRC Press, 908 p., Second Edition, ISBN 0-8493-9126-1, 1998.
- [2] BANGASH, M. Y. H., *Concrete and concrete structures: numerical modeling and applications*, Barking: Elsevier science publishers Ltd., ISBN: 1-85166-294-4, 1989.
- [3] LUNGGREN, K., GUSTAVSON, R., MAGNUSSON, J., “Finite element modelling as a tool to understand the bond mechanisms”, In: *Bond in concrete: from research to standards*, Budapest, 2002.
- [4] FERGUSON, P. M., *Reinforced concrete fundamentals*, Fourth Edition, ISBN: 0-471-01459-1, 1979.
- [5] ROTTS, J. G., *Bond of reinforcement*, In: *Fracture mechanics of concrete structures: from theory to applications*, Report of the Technical Committee 90-FMA Fracture Mechanics to Concrete – Applications, RILEM, Suffolk: St. Edmund Press Ltd, ISBN: 0-412-30680-8, cap. 12, pp. 245-262, 1989.
- [6] AL-JAHDALI, F. A., WAFI, F. F., SHIHATA, S. A., *Development length for straight deformed bars in high-strength concrete*, In: Report SP-149 - Special Publication (ACI), v. 149, October, 1994.
- [7] KWANK, H.-G., KIM, S.-P. “Bond-slip behavior under monotonic uniaxial loads”, *Engineering Structures*, v. 23, p. 298-309, 2001.
- [8] FUSCO, P. B., *Técnicas de armar as estruturas de concreto* (in portuguese), PINI, São Paulo, SP, Brazil, 1995.
- [9] DÉSIK, J., ROMDHANE, M. R. B., ULM, F.-J., FAIRBAIN, E. M. R., “Steel-concrete interface: revisiting constitutive and numerical models”, *Computers and Structures*, v. 71, p. 489-503, 1999.
- [10] SALARI, M. R., SPACONE, E. “Finite element formulations of one dimensional elements with bond-slip”, *Engineering Structures*, v. 23, pp. 815-826, 2001.
- [11] KWAK, H.-G., FILIPPOU, F. C., “Nonlinear FE analysis of R/C structures under monotonic loads”, *Computers and Structures*, v. 65, n. 1, pp. 1-16, 1997.

- [12] YANKELEVSKY, D. Z., “A two-phase one dimensional model for steel-concrete interaction”, *Computers and Structures*, v. 65, n. 6, pp. 781-794, 1997.
- [13] GIRARD, C., BASTIEN, J., “Finite element bond-slip model for concrete columns under cyclic loads”, *Journal of Structural Engineering*, ASCE, v. 128, n. 12, pp. 1502-1510, 2002.
- [14] KOTSOVOS, M. D., PAVLOVIC, M. N., *Structural concrete: finite-element analysis for limit-state design*, Trowbridge: Thomas Telford, Redwood Books, 1st Edition, 559 p., ISBN: 0-7277-2027-9, 1995.
- [15] DEHESTANI, M., MOUSAVI, S.S., “Modified steel bar model incorporating bond-slip effects for embedded element method”, *Construction and Buildings Materials*, v. 81, pp. 284-290, 2015.
- [16] HASKETT, M., OEHLERS, D. J., ALI, M.S.M., “Local and global bond characteristics of steel reinforcing bars”, *Engineering Structures*, v. 30, pp. 376-383, 2008.
- [17] BRISOTTO, D.S., BITTENCOURT, E., BESSA, V. M. R. d’A., “Simulating bond failure in reinforced concrete by a plasticity model”, *Computers and Structures*, v. 106-107, pp. 81-90, 2012.
- [18] ANSYS, on-line manuals, Engineering Analysis System, 2008.
- [19] FERNANDES, R. M., *The influence of repeated loads on the steel-concrete bond* (in portuguese), Master degree, SET/EESC/USP, São Carlos, SP, Brazil, 2000.
- [20] POPOVICS, S., “A numerical approach to the complete stress-strain curves for concrete”, *Cement and concrete research*, v. 3, n. 5, pp. 583-599, 1973.
- [21] RILEM-FIP-CEB, “Bond test for reinforcing steel: 1-Beam test (7-II-28 D). 2-Pullout test (7-II-128): Tentative recommendations”, *Materials and Structures*, v. 6, n. 32, pp. 96-105, 1973.
- [22] ALMEIDA FILHO, F. M.; De NARDIN, S.; EL DEBS, A. L. H. C., “Interface aço-concreto: análise dos parâmetros do contato e sua influência na simulação via MEF” (in portuguese). In: *XXV CILAMCE: Iberian Latin American Congress on Computational Methods*, 16p., Recife-PE, Brasil, 2004.
- [23] DE NARDIN, S., ALMEIDA FILHO, F. M., EL DEBS, A. L. H. C., “Non-linear analysis of the bond strength behavior on the steel-concrete interface by numerical models and pull-out tests”, In: *ASCE Conference - Structures 2005*, 12 p., v. 171, New York, USA, 2005.
- [24] DE NARDIN, S., ALMEIDA FILHO, F. M., EL DEBS, A. L. H. C., EL DEBS, M. K., “Steel-concrete interface: influence of contact parameters”, In: *FIB International Conference: “Keep concrete attractive”*, 6p., Budapest, Hungary, 2005.
- [25] ALMEIDA FILHO, F. M. *Contribution to the study of the bond between steel bars and self-compacting concrete* (in portuguese), Doctoral Thesis, 310p, SET/EESC/USP, São Carlos, SP, Brazil, 2006.
- [26] ZHOU, B., WU, R., FENG, J., Two models for evaluating the bond behavior in pre- and post-yield phases of reinforced concrete”, *Construction and Buildings Materials*, v. 147, pp. 847-857, 2017.

ORCID

Fernando Menezes de Almeida Filho <http://orcid.org/0000-0002-6927-6377>
Silvana De Nardin <http://orcid.org/0000-0002-8736-4987>
Ana Lúcia Homce de Cresce El Debs <http://orcid.org/0000-0001-6359-7674>